Surface Investigation, 2000, Vol. 15, pp. 1127–1134
Reprints available directly from the publisher
Photocopying permitted by license only

Atomic Force Microscopy Visualization of RNA and Ribonucleotides of the Tobacco Mosaic Virus

M. O. Gallyamov[1], Yu. F. Drygin[2], and I. V. Yaminsky[3]

[1]*Physical Department, M. V. Lomonosov Moscow State University, Moscow, Russia*
[2]*A. N. Belozerskii Research Institute of Physicochemical Biology, M. V. Lomonosov Moscow State University, Moscow, Russia*
[3]*Chemical Department, M. V. Lomonosov Moscow State University, Moscow, Russia*

Received 4 April, 1998

High-molecular weight virus RNA on the surfaces of various substrates has been studied by atomic force microscopy (AFM). The process of releasing virus RNA from the protein shell under the action of chemical reagents has been studied. Special attention has been paid to the procedure of the preparation of samples and the immobilization of the structures under study. Images of the starting virus particles, partially deproteinized virus structures, and completely released RNA have been obtained. The images obtained have been statistically processed. The factors restricting the spatial resolution of the SFM patterns of the structures under study have been analysed.

INTRODUCTION

Scanning probe microscopy (SPM) (including atomic force microscopy [1], scanning tunnelling microscopy (STM) [2], and others) made it possible to study the structures and conformational properties of macromolecules of nucleic acids and their complexes under conditions close to native [3, 4]. New information on the morphology of DNA complexes with surfactants was obtained [5]. The use of SPM for physical mapping of nucleic acids [6] and their interaction with proteins [7, 8] is a prominent demonstration of the possibilities of the method.

Various methods for the immobilization of macromolecules of linear DNA, circular plasmidic DNA, and two-chain RNA on the surfaces of various substrates for SPM studies have been developed presently [9–12]. At the same time, the works devoted to the SPM study of high-molecular weight one-chain RNA are virtually lacking [13]. This is explained by the specificity of a molecule of one-chain RNA (the absence of the double spiral) and, as a consequence, a lower "rigidity," which impedes the immobilization of this macromolecule in the extended state on the substrate.

The procedure of the preparation of RNA in the extended state for studies by electron microscopy includes the formation of an RNA complex with proteins (cytochrome C or diisopropyl phosphate trypsin) at the air–water interface and the consequent transfer of this complex to the solid substrate surface. Evidently, in this case, the protein "coat" restricts the solution of problems related to the fine structure of RNA.

The observation of free RNA makes it possible both to perform the physical mapping of elements of the secondary RNA structure and to study its specific interaction with proteins which recognize specific (for example, regulatory) sequences of nucleotides. The study of the interaction of virus DNA and proteins can give a contribution to the understanding of the mechanisms of aggregation and reproduction of viruses, structural organization and functioning of ribonucleoproteides.

This work is devoted to the development of methods of the preparation of virus RNA and ribonucleoproteides for SPM studies.

EXPERIMENTAL

Solutions were prepared with deionized bidistilled water. The preparation of the virus (BTM, strain U1) obtained by the differential centrifuging method and centrifuging in the gradient of the density of a sucrose solution was kindly presented by E. N. Dobrov (Moscow State University).

Virus particles were deproteinized as follows: (1) with a 72% solution of dimethyl sulfoxide (DMSO) [14] (30-min exposure), (2) with a 4 M solution of urea [15] (2.5-h exposure), and (3) with a solution of glycine with pH 10.4 [16] (3-h exposure).

Both clean (a fresh cleave) and modified surface of high-orientation pyrolytic graphite (pyrographite) and mica were used as substrates. The modification was the treatment of the surface with a cationic surfactant, benzyl dimethyl alkylammonium chloride (BAC). The modification process (exposure to a 1% solution of BAC in formamide [17]) was completed by washing with water and drying in a jet of the filtered compressed air.

Adsorption of the structures under study was performed from a drop of the preparation, which was deposited on the substrate surface and exposed to a moist medium under a cap. The duration of exposure was varied from several seconds to an hour and more. After the end of exposure, the substrate surface was washed with water and dried in a jet of the filtered compressed air.

AFM studies were carried out on a Nanoscope-III instrument (Digital Instruments, USA) in the air in the constant force mode and tapping mode contacts. For the studies in the constant force mode, cantilevers with a rigidity of 0.06 N/m with a silicon nitride microprobe were used. Cantilevers with a resonance frequency of 350–380 kHz and silicon microprobes were used for the studies in the tapping mode contact.

RESULTS AND DISCUSSION

Scanning probe microscopy of virus particles. Particles of the tobacco mosaic virus were studied in the constant force and tapping contact modes on the pyrographite and mica surfaces. It was found that the rate of sorption of virus particles on the fresh cleave of the

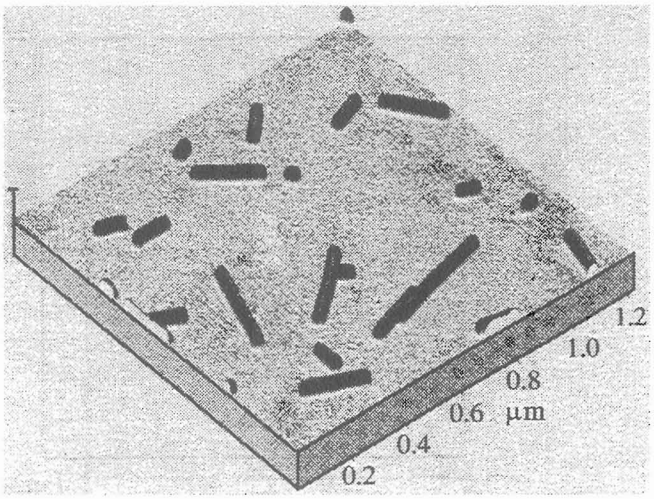

Figure 1. Particles of the tobacco mosaic virus adsorbed on the pyrographite surface. AFM study, the height was measured in the tapping contact regime.

surface was much higher for the pyrographite substrate than that for the mica substrate. In the first case, under equal conditions of sorption (temperature, volume concentration of viruses in the preparation, time of washing, etc.), the surface density of virus particles was much higher. At the same time, on the pyrographite substrate during scanning in the constant force contact mode, the virus particles are unstable and withdrawn with a tip even when the acting force is minimized to a value lower than 1 nN. Stable AFM patterns of virus particles on pyrographite can be obtained only in the tapping mode of contact. In the case of the mica surface, the adhesion force of the virus particles is sufficient for the studies in the constant force mode of contact with an acting force of ~10 nN.

A high rate of sorption of virus particles on the pyrographite surface, as compared to that on mica, can be explained by the influence of the hydrophobic effect. This assertion is favored by the fact that the sorption rate of the virus particles increases if the mica surface is hydrophobized by the treatment with BAC.

At the same time, instability of the virus particles adsorbed on pyrographite in the constant force contact mode is explained by a weak adhesion of the particle due to the inertness of the substrate (the hydrophobic effect does not contribute to the adhesion force when the studies are performed in air, because it is manifested only in an aqueous medium).

The AFM patterns of particles of the tobacco mosaic virus are presented in Fig. 1. According to the analysis of the data, for the virus particles, the maximum of the Gauss approximation of the length distribution corresponds to 320 nm, the average length is 310 nm, and the mean-square relative deviation from the average value is 30% (the number of the analyzed AFM patterns of the viruses $N = 120$). Such a wide distribution is explained, first, by the partial destruction of the virus structures during centrifuging and, second, by the edge-to-edge aggregation of the virus particles. In the beginning of the treatment of the

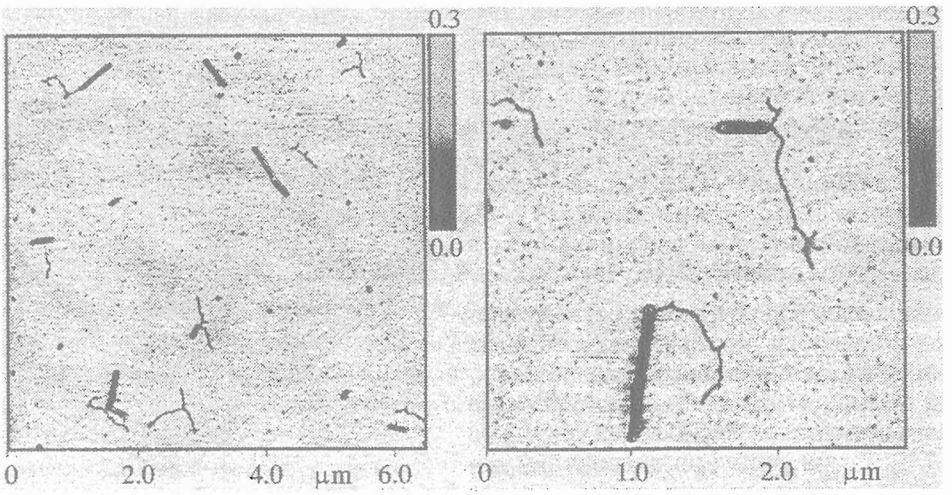

Figure 2. Virus structures partially deproteinized by the treatment with 72% DMSO and adsorbed on mica. AFM study, the friction forces were measured in the constant force contact mode.

virus structures in order to release virus RNA, the maximum of the length distribution of the virus particles is shifted to a shorter-wave region. For example, for the virus particles treated with 50% formamide for 2 min, the maximum is 260 nm ($N = 500$), and for those treated with 40% DMSO at 37° for 30 min, the value of the maximum is 180 nm ($N = 270$).

The analysis of the heights of the AFM patterns of the virus particles above the substrate surface gives a value of 18±2 nm (regardless of the mode of the study), which agrees well with the published data [18].

The BTM particles, being natural "nanometric" objects with rigidly fixed geometric parameters (each particle is a cylinder 300 nm in length and 9 nm in radius), can serve as a convenient test-object for analysis of the quality of a probing tip. A similar analysis makes it possible to follow the mechanism of the appearance of artifacts, for example, in the study of virus RNA. According to elementary geometric considerations for a tip with the radius of the end curvature R, the value of the really measured width at the half-height of the AFM patterns of the virus particles with the radius r should be the following:

$$d_{\text{eff}} = 2(2Rr + r^2)^{1/2}. \tag{1}$$

The experimentally determined values of the width of the AFM patterns of virus particles for the tapping and constant force contact modes are 30±5 nm ($N = 270$) and 32±6 nm ($N = 400$), respectively. Using formula (1), we can estimate the curvature radius for probe tips of the cantilevers of the used types: $R \approx 6-7$ nm.

Scanning probe microscopy of deproteinized virus structures with partially released RNA macromolecules. Under mild conditions of deproteinization, ribonucleoproteides

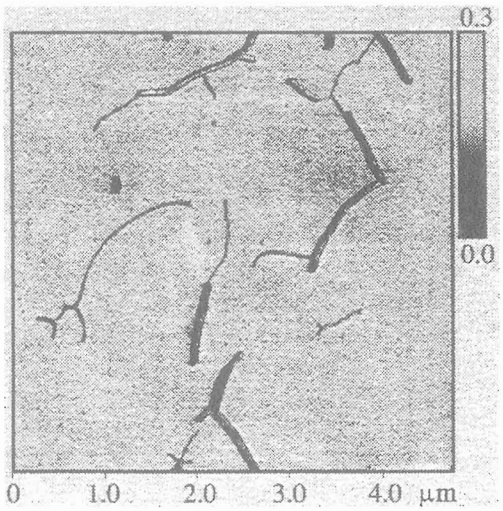

Figure 3. Virus structures partially deproteinized by the treatment with a 4 M solution of urea and adsorbed on mica. AFM study, the friction forces were measured in the constant force contact mode.

(RNP) with shifting (from one or both ends) RNA filaments were observed (Figs. 2 and 3). Comparative analysis of three methods used for the partial polar deproteinization of BTM and release of RNA showed that the method using DMSO is the most promising (Fig. 2). The deproteinization method in solutions with an alkaline pH value is characterized by a great background of the observed AFM patterns. In addition, in this case, RNA molecules tend to aggregation. The method using urea makes it possible to obtain AFM patterns with an insignificant background, but the aggregation of virus RNP is observed in this case (Fig. 3).

Scanning probe microscopy of virus RNA molecules. At the final stage of the treatment of virus particles, the protein shell is decomposed, and the RNA molecule is completely released. The typical results of the AFM study of free RNA adsorbed on the mica surface are presented in Fig. 4.

The analysis of the width of RNA macromolecules adsorbed on mica gives values of 10–15 and 20–30 nm for the tapping and constant force contact modes, respectively.

Let us use formula (1) for the estimate of the broadening mechanism related to the finiteness of the curvature radius of the probe. Based on the analysis of the length distribution of free macromolecules (see below) and knowing the number of nucleotides in the molecule (~6400), let us estimate the radius of the RNA macromolecule: $r \approx 1$ nm; for the probe radius, we use the values estimated above: $R \approx 6–7$ nm. Then the actually measured width at the half-height of the AFM pattern should be 7–8 nm. This estimate differs from the experimentally observed value likely due to deformations of the sample under the probe action. The role of these deformations is much higher for the constant force mode as compared to that for the tapping contact mode.

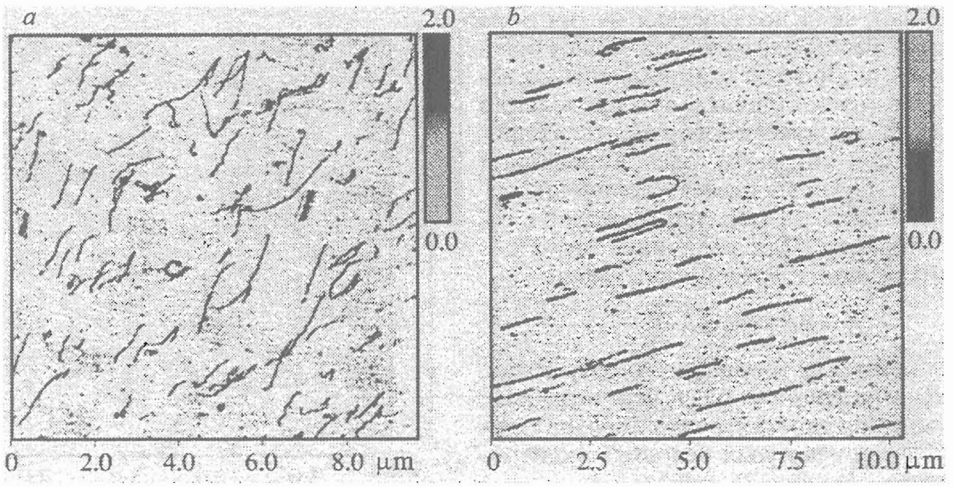

Figure 4. RNA molecules released from the protein shell by the treatment with DMSO and adsorbed on mica with different degrees of orientation along the flow (*a*, *b*). AFM study, the height was measured in the constant force contact mode.

In fact, the action force on the sample caused by the bent of the cantilever can be minimized during scanning to 10^{-9} N and lower. However, when the studies are carried out in the air, the surface of hydrophilic samples is covered with the adsorbed water film, which results in an increase in the action force of the probe on the sample due to the capillary effect. For this additional force action, we have

$$F = 4\pi R\gamma\cos\Theta,$$

where R is the curvature radius of the probe, γ is the surface tension of water at the interface with air, and Θ is the contact angle for the material of the sample (probe) and water. Under standard experimental conditions, the following estimate is valid: $F \approx 10^{-8}$ N.

When the probe of the R radius acts with the F force on the RNA macromolecule of the r radius, the probe, sample, and substrate are deformed. The approach h of the probe and sample (as well as that of the sample and substrate) can be estimated using the contact Hertz theory [19]:

$$h \approx (FD)^{2/3}((R+r)/2)^{-1/3}, \tag{2}$$

where

$$D = \frac{3}{4}((1-\sigma^2)/E + (1-\sigma'^2)/E').$$

Here E' and σ' are the Young modulus and the Poisson coefficient for the probe (substrate)

materials, E and σ are the same parameters for an elastic rod which approximates the RNA macromolecule.

The region of contact of the probe and macromolecule is an ellipse with semi-axes a and b:

$$a \equiv (FD)^{1/3}((R+r)/2)^{-2/3}R$$

$$b \equiv (FD)^{1/3}((R+r)/2)^{-2/3}r\,.$$

Assuming that $E' >> E$ (the Young moduli of silicon and silica range from 100 to 150 GPa), let us take into account the contribution of only the first term to D. Then estimating $E \approx 10$ GPa, we obtain the estimate of 3 nm and 0.3 nm for a and b, respectively. Thus, the lateral sizes of the region of the probe–sample contact are comparable with the radius of RNA. It is evident from the presented estimate that the deformation of bio-objects should be taken into account for the analysis of the AFM patterns. Thus, the lateral sizes of the contact region determine the limit of the accessible spatial resolution.

Based on formula (2), we obtain $h \approx 0.5$ nm. Thus, for the relative decrease of the heights of RNA macromolecules above the substrate surface we obtain an estimate of 50%, which agrees well with the obtained experimental results. This justifies the use of the estimate for the Young modulus of the rod which models RNA ($E \approx 10$ GPa).

The experimental analysis of the values of the heights of macromolecules showed that they varied sufficiently strongly for both different molecules and different regions of the same molecule and mainly range within 0.3–1.5 nm (for the studies in both the constant force and tapping contact modes). This scatter can be explained by the retention of elements of the secondary structure by the macromolecule (incomplete unfolding on the substrate surface, the presence of twisted regions).

The presence of loops and "pins" also indicates the partial retention of elements of the secondary structure of the macromolecules. The unfolding of macromolecules can be favored by the deposition on the substrate in a flow (Fig. 4*b*). The regions of immobilization of the macromolecule on the substrate are distinctly identified on the AFM patterns. It can be seen that the molecule, being immobilized at a specified point, is oriented unfolding along the flow. The stabilization of macromolecules in the unfolded state on the substrate surface makes it possible to analyze the length distribution of RNA molecules. According to our results, for RNA macromolecules released using DMSO, the maximum of the length distribution is 1.6±0.5 μm. Taking into account that RNA BTM of the U1 strain contains about 6400 nucleotides, we can determine the length of the internucleotide bond for RNA whose images were obtained under the conditions described by us. This value is 0.25±0.08 nm.

The authors thank E. N. Dobrov (Moscow State University) for the kindly presented preparation of the virus. This work was supported in part by the Russian Foundation for Basic Research, project nos. 97-04-49763 and 97-03-32778a.

REFERENCES

1. G. Binnig, C. F. Quate, and Ch. Gerber, *Phys. Rev. Lett.*, **56**: 930 (1986).
2. G. Binnig and H. Rohrer, *Helv. Phys. Acta*, **55**: 726 (1982).
3. Y. L. Lyubchenko, A. A. Gall, L. S. Shlyakhtenko, *et al.*, *J. Biomol. Struct. Dynam.*, **10(3)**: 589 (1992).
4. C. Bustamante, J. Vesenka, C. L. Tang, *et al.*, *Biochemistry*, **31**: 22 (1992).
5. V. G. Sergeyev, O. A. Pyshkina, M. O. Gallyamov, *et al.*, *Progr. Colloid. Polym. Sci.*, **106**: 978 (1997).
6. M. N. Murray, H. G. Hansma, M. Bezanilla, *et al.*, *Proc. Natl. Acad. Sci. USA*, **90**: 3811 (1993).
7. M. Guthold, M. Bezanilla, D. A. Erie, *et al.*, *Proc. Natl. Acad. Sci. USA*, **91**: 12927 (1994).
8. W. A. Rees, R. W. Keller, J. P. Vesenka, *et al.*, *Science*, **260**: 1646 (1993).
9. N. H. Thomson, S. Kasas, B. Smith, *et al.*, *Langmuir*, **12**: 5905 (1996).
10. Y. L. Lubchenko, B. L. Jacobs, and S. M. Lindsay, *Nucleic Acids Res.*, **20**: 3983 (1992).
11. M. O. Gallyamov and I. V. Yaminsky, *Scanning Probe Microscopy of Biopolymers*, (Moscow: Nauchnyi Mir) (1997) (in Russian).
12. A. Schaper, L. I. Pietrasanta, and T. M. Jovin, *Nucleic Acids Res.*, **21**: 6004 (1993).
13. Yu. F. Drygin, O. A. Bordunova, M. O. Gallyamov, and I. V. Yaminsky, *FEBS Lett.*, **425**: 217 (1998).
14. A. Nikolaieff, G. Lebeurier, M.-C. Morel, and L. Hirth, *J. Gen. Virol.*, **26**: 295 (1975).
15. L. E. Blowers and T. M. A. Wilson, *J. Gen. Virol.*, **61**: 137 (1982).
16. R. Hogue and A. Asselin, *Can. J. Botany*, **62**: 2236 (1984).
17. H. J. Vollenweider, J. M. Sogo, and Th. Koller, *Proc. Natl. Acad. Sci. USA*, **72**: 83 (1975).
18. G. Lebeurier, A. Nicolaieff, and K. E. Richards, *Proc. Natl. Acad. Sci. USA*, **74**: 149 (1977).
19. L. D. Landau and E. M. Lifshits, *Elasticity Theory*, (Oxford: Pergamon) (1987).